5-3-2008

Optimization of the material selection process for cryogenic composite overwrapped pressure vessels

Mark Vernon Dyess

OPTIMIZATION OF THE MATERIAL SELECTION PROCESS FOR CRYOGENIC COMPOSITE OVERWRAPPED PRESSURE VESSELS

By

Mark Vernon Dyess

A Thesis
Submitted to the Faculty of
Mississippi State University
in Partial Fulfillment of the Requirements
for the Degree of Masters of Science
in Mechanical Engineering
in the Department of Mechanical Engineering

Mississippi State, Mississippi

May 2008

OPTIMIZATION OF THE MATERIAL SELECTION PROCESS FOR CRYOGENIC COMPOSITE OVERWRAPPED PRESSURE VESSELS

By

Mark Vernon Dyess

Approved:

Judy Schneider Associate Professor of Mechanical Engineering (Director of Thesis)	Anthony J. Vizzini Professor and Department Head of Aerospace Engineering (Committee Member)
Rani W. Sullivan Assistant Professor of Aerospace Engineering (Committee Member)	Steven R. Daniewicz Professor and Graduate Coordinator of Mechanical Engineering

Glenn Steele
Interim Dean and Professor
Bagley College of Engineering

Name: Mark Vernon Dyess

Date of Degree: May 02, 2008

Institution: Mississippi State University

Major Field: Mechanical Engineering

Major Professor: Dr. Judy Schneider

Title of Study: OPTIMIZATION OF THE MATERIAL SELECTION PROCESS FOR CRYOGENIC COMPOSITE OVERWRAPPED PRESSURE VESSELS

Pages in Study: 53

Candidate for Degree of Masters of Science

The objective of this research was to develop a test methodology for the evaluation of materials for possible use in cryogenic composite overwrapped pressure vessels (COPVs). This paper investigates various micromechanical and macromechanical techniques to test the interaction between fibers and resins. Uniaxial tension testing was performed at ambient and cryogenic temperatures on neat resin samples, straight-sided composite specimens, and NOL ring specimens. COPVs were constructed and burst tested to provide a performance comparison. Results show resins suitable for use at cryogenic conditions display a LN_2 temperature elongation to failure greater than 2% and an ambient temperature elastic modulus less than 35 MPa. NOL rings were determined to be the preferred composite test method rather than straight-sided specimens. Mechanical performance of the NOL rings compares well with actual COPV performance.

DEDICATION

I would like to dedicate this research to my parents, Jim and Theresia Dyess, and my brother Matt. Without their ever-present encouragement and support, this work would not have been possible.

ACKNOWLEDGEMENTS

The author expresses his sincere gratitude to the many people whose selfless assistance made this thesis possible. First, I would like to thank my major professor Dr. Judy Schneider. Her enthusiasm and whip-cracking ability ensured me the guidance and resources that carried my research forward. Throughout my thesis-writing period, she provided encouragement, immediate feedback, and invaluable suggestions. Appreciation is also due to the other members of my thesis committee for their constructive comments and guidance. Thanks to Mr. Tom DeLay at the NASA Marshall for his endless support. He made sure that my summer at NASA was not just a work experience, but a learning one. Finally, thanks to Mr. Calvin Walker. His composites wisdom, and willingness to share it, was my stepping stone into a field of great potential. This research was financially made possible by the following contracts: NCAM-LP # NCC8-223 (MSU), NASA-STTR Phase I Contract #NNM05AA61C (HEI/MSU), and NASA-SBIR Phase II Contract # NNM05AA45C (HEI/MSU).

TABLE OF CONTENTS

DEDICATION ii

ACKNOWLEDGEMENTS iii

LIST OF TABLES vi

LIST OF FIGURES vii

CHAPTER

1. INTRODUCTION 1

2. COPV MANUFACTURING AND MATERIALS 5

2.1 Filament Winding Process 6
2.2 COPV Constituents 9
2.2.1 Fibers 9
2.2.2 Resins 10
2.2.3 Fiber Sizing 11

3. EVALUATION OF CONSTITUENT COMPATIBILITY 13

3.1 Interfacial Shear Strength (IFSS) Testing 13
3.1.1 Single Fiber Pull-Out Test 14
3.1.2 Microbond Test 15
3.1.3 Fragmentation Test 16
3.1.4 Indentation Test 17
3.2 Wettability Testing 18
3.3 Composite Coupon Testing 19
3.3.1 Straight-sided Specimen 19
3.3.2 NOL Ring Specimen 20
3.4 Tank Testing 21

4. EXPERIMENTAL PROCEDURE 22

4.1 Neat Resin Specimen 23
4.2 Neat Resin Testing 25
4.3 Straight-sided Specimen 26
4.4 Straight-sided Specimen Testing 27
4.5 NOL Ring Specimen 28
4.6 NOL Ring Specimen Testing 29
4.7 COPV Fabrication 30
4.8 COPV Burst Testing 31

5. RESULTS AND DISCUSSION 33

5.1 Neat Resin Testing Results 33
5.2 Fiber Sizing Affect on UTS 36
5.3 NOL Ring Width Affect on UTS 38
5.4 NOL Ring and Straight-sided Comparison 39
5.5 NOL Ring and COPV Comparison 41

6. CONCLUSIONS AND FUTURE WORK 43

REFERENCES 46

APPENDIX

MEASURED MATERIAL PROPERTY VALUES 50

LIST OF TABLES

2.1 Summary of various fibers and properties 10

4.1 Curing conditions for resin systems 24

A.1 Resin properties at ambient temperature tested at 0.127 cm/min crosshead velocity 51

A.2 Resin properties at ambient temperature tested at varying crosshead velocities in accordance with ASTM D 638 51

A.3 Resin properties at LN_2 temperature 51

A.4 Resin properties at LH_2 temperature 52

A.5 Strength of 2.5 cm wide NOL rings with various resins and IM7 fiber [43] 52

A.6 Strength of 2.5 cm wide NOL rings with various resins and IM7 fiber with various sizings tested at ambient conditions 52

A.7 Strength of 2.5 cm wide NOL rings with various resins and IM7 fiber with various sizings tested at LN_2 conditions 52

A.8 T-1000/HEI 535 composite strength comparison for 0.9 cm and 2.5 cm wide NOL rings 53

A.9 T-1000/Epon 828/W composite strength comparison for 0.9 cm wide NOL ring and straight-sided specimens at ambient conditions 53

A.10 T-1000/Epon 828/W composite strength comparison for 0.9 cm wide NOL ring and straight-sided specimens at LN_2 conditions 53

LIST OF FIGURES

1.1 Potential weight savings for ARES upper stage GHe pressurant tanks using cryogenic COPVs. Cylindrical 92 liter COPVs were designed using high performance candidate materials for cryogenic application at 31.4 MPa operating pressure with a 47 MPa minus 3σ burst pressure rating [2] 2

2.1 Cut-away picture of typical COPV. Metal liner may be treated to to either promote or prevent adhesion to overwrap 5

2.2 Strength and stiffness of composite materials and metals [7] 6

2.3 Filament winding process schematic [10] 7

2.4 Filament winding axes of motion [11] 8

2.5 Entec filament winding system at the NASA-MSFC facility 9

2.6 Role of fiber sizing/finish [22] 11

3.1 Single fiber pull-out test method 14

3.2 Microbond test method 15

3.3 Fragmentation test method 16

3.4 Indentation test method 17

3.5 Typical composite straight-sided specimen geometry [31] 19

3.6 NOL ring split-D loading device 21

4.1 (a) Modified dog bone geometry (dimensions are in inches) and (b) results of FEA showing stress distributed over the gage section [21] 23

4.2 Overview of LN_2 temperature tension testing facility at MSU. (a) MTS extensometer attached to specimen mounted in grips, (b) interior of cryostat, and (c) cryostat mounted on Instron load frame 25

4.3 Straight-sided specimen in bolted grips 28

4.4 Close up of split-D test fixture. (a) Prior to submersion in LN_2 and (b) after completion of test 30

4.5 (a) Schematic of LN_2 burst test and (b) the NASA's LN_2 burst facility 32

5.1 Ultimate tensile strength of resins tested at ambient, LN_2, and LH_2 34

5.2 Elongation to failure of resins tested at ambient, LN_2, and LH_2 34

5.3 Modulus of elasticity of resins tested at ambient, LN_2, and LH_2 35

5.4 Strength of 2.5 cm wide NOL rings with various resins and IM7 fiber [43] 35

5.5 Strength of 2.5 cm wide NOL rings with various resins and IM7 fiber with various sizings 37

5.6 T-1000/HEI 535 composite strength comparison for 0.9 cm and 2.5 cm wide NOL rings 38

5.7 T-1000/Epon 828/W composite strength comparison for 0.9 cm wide NOL ring and straight-sided specimens 40

5.8 Delivered fiber strength for various resin systems with IM7 fiber based on (a) 2.5 cm wide NOL ring tests and (b) COPV burst tests [2] 42

CHAPTER 1

INTRODUCTION

As the field of polymeric composites becomes better understood, the potential areas of application are increasing. The high strength-to-weight ratio of polymeric composite overwrapped pressure vessels (COPVs) benefits many light weight, high pressure applications such as fuel storage and pressurant tanks. For instance, the NASA's new ARES launch vehicles will likely utilize a bank of gaseous helium (GHe) pressure vessels located inside the liquid hydrogen (LH_2) tank to assist with operational issues, a concept that was used in the Apollo program [1]. For the Apollo program, these tanks were 92 liter titanium spheres, weighing approximately 26.8 kg each. Figure 1 explores the potential weight savings in this particular application if COPVs were used [2].

The applications for storage of cryogenic fuels includes: liquid methane at 109 K, liquid oxygen (LOX) at 90 K, and LH_2 at 20 K. However, with the introduction of a material to a new environment it is necessary to understand the resulting change in material behavior. Because many of these fuels are flammable, the use of liquid nitrogen (LN_2) at 77 K provides a safe, low cost environment for initial evaluation.

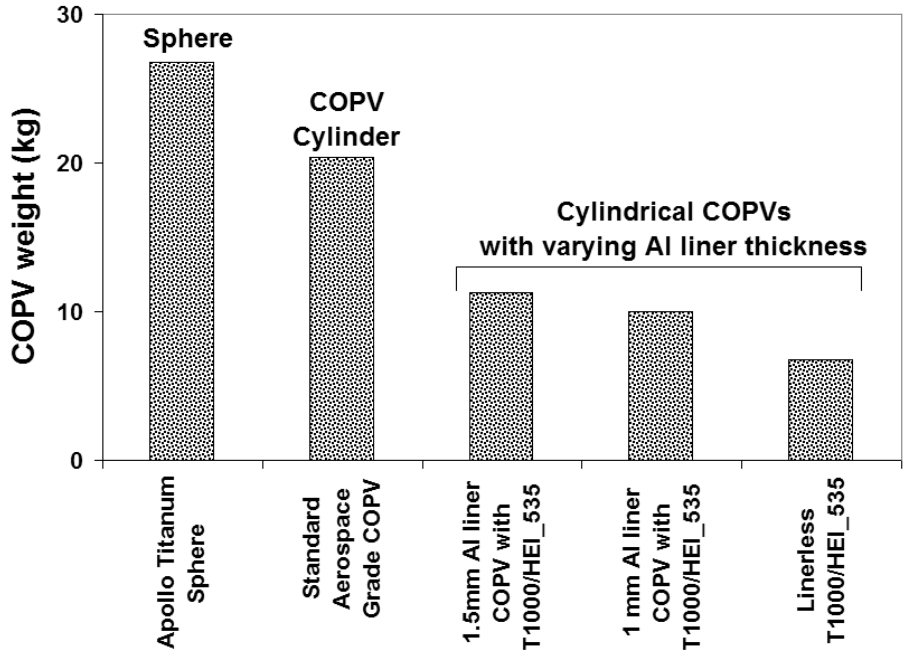

Figure 1: Potential weight savings for ARES upper stage GHe pressurant tanks using cryogenic COPVs. Cylindrical 92 liter COPVs were designed using high performance candidate materials for cryogenic application at 31.4 MPa operating pressure with a 47 MPa minus 3σ burst pressure rating [2]

The most direct method of evaluating the behavior of a COPV at cryogenic temperatures would be to perform actual tank burst tests. However, with such a wide variety of options for the fiber and matrix selection, COPV testing is often cost prohibitive, even using subscale tanks. Instead, a more systematic approach is needed. By performing small scale testing of composites and their constituents and then relating these results to actual tank burst performance, it may be possible to develop guidelines for the down selection of potential components, and thus optimize the design of COPVs.

The purpose of this research project is to evaluate various test methods in order to develop a more efficient method of selecting viable composite systems for use at cryogenic conditions. Volume 15.3 of the ASTM standards [3] provides guidelines for composite evaluation at ambient and high temperature environments. Although not specifically for cryogenic temperature testing, some test methods are provided for neat resin testing that distinguish between procedures for specimens above and below the glass transition temperature [4]. However, many of the ambient temperature methods may still be applicable at cryogenic temperatures and are thereby used for initial conditions and modified as needed to facilitate testing.

The methodology of the MIL-17-handbook [5] was used as a baseline to establish a method for composite constituent screening. Initially, the neat resin matrix materials are tested in uniaxial tension to determine their mechanical properties at ambient, LN_2, and LH_2 temperatures. Once suitable fibers and neat resins are identified, the compatibility of the various combinations needs to be verified. This evaluation may include micromechanical testing of the interface, fiber wettability studies, or macromechanical testing of the composite itself. Using this data, actual COPVs (full scale or subscale) can be designed and subjected to burst testing to ensure that the results of small scale composite and constituent testing are meaningful.

Chapter 2 will give an overview of the basic manufacturing process for COPVs, including a discussion of the materials involved and their desired properties. Chapter 3 reviews published techniques for determining fiber/matrix compatibility, including an evaluation of the practicality of each method subjected to cryogenic conditions.

Chapter 4 describes the experimental procedures that were followed to evaluate the various materials in this study. The results are presented in Chapter 5 with a discussion of the conclusions and recommended future work in Chapter 6.

CHAPTER 2

COPV MANUFACTURING AND MATERIALS

Traditional pressure vessels have been built out of metals such as titanium, steel, and aluminum. Figure 2.2 shows a comparison of strength vs stiffness for several composite materials and metals. The values have been normalized by dividing each material's properties by its corresponding density. As shown, metal tanks may be unfavorable for applications that are weight sensitive. On the other end of the scale you have linerless, composite tanks. These tanks can be up to 58% lighter, but concerns over the possibility of microcracking and permeability tend to prevent their application [6]. Thus COPVs provide an attractive middle ground. A thin metal liner creates a barrier to gas permeability, while the composite overwrap satisfies the structural requirements. The resulting vessel provides a suitable option for applications such as fuel storage and pressurant tanks.

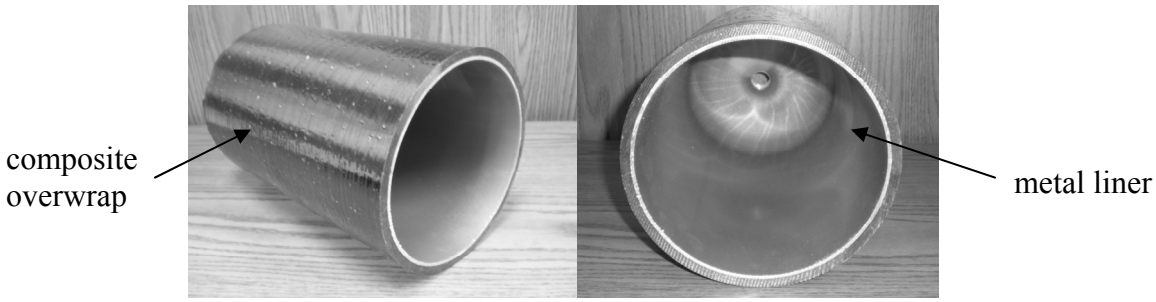

Figure 2.1: Cut-away picture of a COPV. Metal liner may be treated to either promote or prevent adhesion to overwrap.

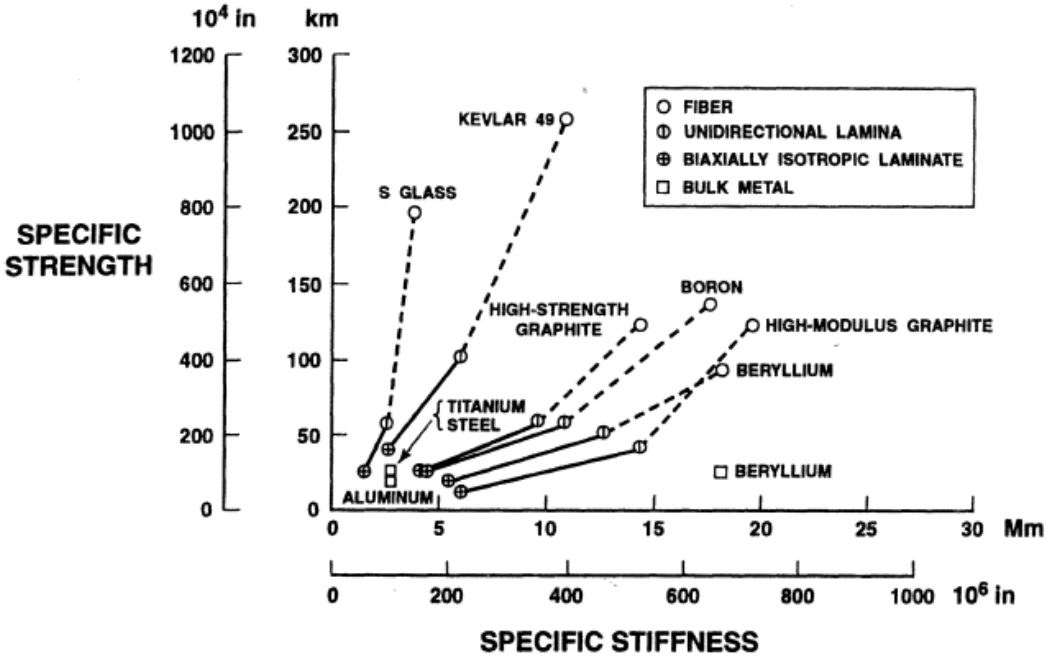

Figure 2.2: Strength and stiffness of composite materials and metals [7]

2.1 Filament Winding Process

A preferred method for manufacturing structures of revolution, such as cylinders or pressure vessels, is filament winding [8,9]. It is a method by which resin-impregnated fibers are wound around a mandrel in a controlled pattern to form the desired part. By varying factors such as wind angle and number of layers, the material is added such that the final part has the specific mechanical characteristics needed.

The process begins with spools of fiber tows. Spools are loaded into a tensioner creel, which monitors the load on each fiber tow and maintains constant tension as the spools unwind. This is an important part of the process as tension can directly affect the fiber volume and void content of the finished part.

Resin is typically added in one of three ways: prepreg, in which the spools of fiber are provided with resin already impregnated into the fiber, through wet winding, in which resin is added during the winding process, or through resin infusion, in which winding is done with dry fibers and then the laminate is saturated with resin through a vacuum transfer process. In the case of wet winding, the fibers are passed through a resin bath system where the tows are "wetted out" with resin. The impregnated fibers pass through a payout eye, located on the carriage of the filament winder, and are fed onto the rotating mandrel. Figure 2.3 illustrates this process.

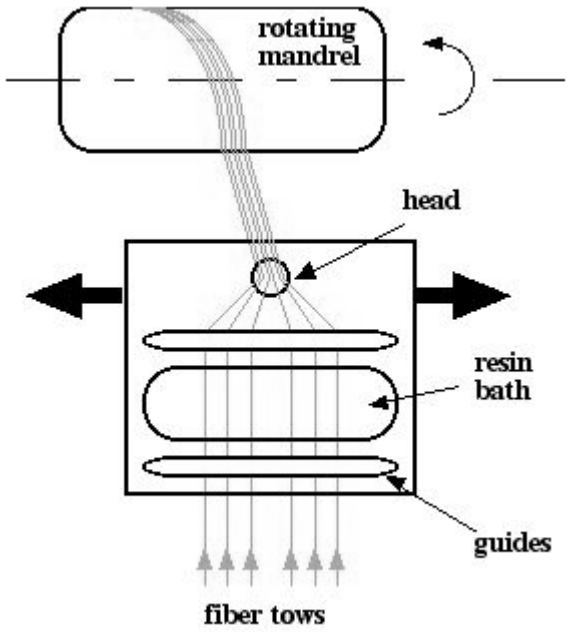

Figure 2.3: Filament winding process schematic [10]

Different winding patterns are achieved through the use of the filament winder's various axes of motion, seen in Figure 2.4. Wind angles from near 0° to near 90° can be achieved. Two of the commonly used winding patterns are helical winding and hoop

winding. In helical winding, the mandrel rotates while the fiber feed carriage moves back and forth at a controlled speed to generate the desired helical angle. This pattern creates a weaving effect and has the appearance of fiber crossovers repeating at certain points along the mandrel. Figure 2.5 shows a helical pattern being wound. Hoop wraps are a high angle winding that approaches 90° (typically ~88° for this study). With each full rotation of the mandrel, the fiber feed carriage advances horizontally one full bandwidth. Hoop wraps are applied only to the cylindrical section of the vessel, while helical wraps are able to reinforce both the cylinder and the domes. Vessels are typically designed such that failure occurs first in the hoop fibers.

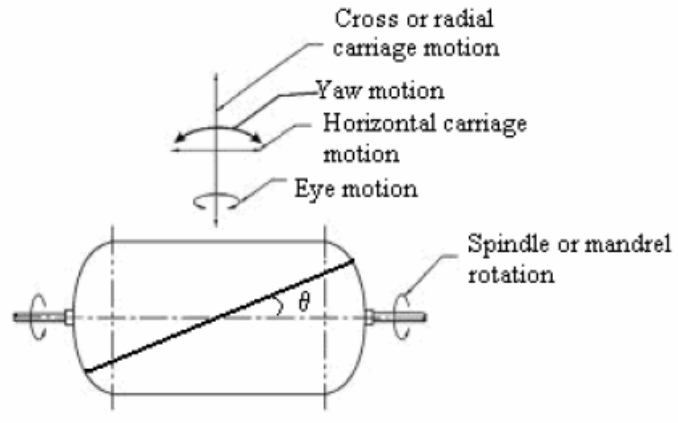

Figure 2.4: Filament winding axes of motion [11]

Figure 2.5: Entec filament winding system at the NASA-MSFC facility

2.2 COPV Constituents

Composites consist of a matrix material and reinforcing fibers. The fibers are responsible for carrying the majority of the load, while the matrix helps distribute load between fibers and protects them from some environmental effects. An additional and sometimes overlooked constituent is the fiber sizing. This interface between the fiber and the matrix can also affect the bulk material properties, as it assists in transfer of load between fibers and resin.

2.2.1 Fibers

In today's market there is a wide variety of fibers available to choose from, such as glass, Kevlar, PBO, and carbon as summarized in Table 2.1. In the case of COPVs, carbon fibers are commonly used as the reinforcing fiber. With the use of an impervious liner, the difference in strain behavior between the liner and overwrap must be noted. A study has been reported for a glass-resin composite cylinder with an aluminum liner which suggested that cyclic damage may occur due to the strain incompatibility between

the two [12]. The desire to minimize this elastic strain incompatibility, suggests an advantage to using a high-modulus fiber such as carbon. A companion study has evaluated fiber properties as a function of environment [13].

Table 2.1: Summary of various fibers and properties

Fiber	E (GPa)	UTS (GPa)	$\varepsilon_{failure}$ (%)
Kevlar 49 [14]	112	3.00	2.4
E-Glass [8]	72	3.45	4.4
PBO (Zylon AS) [15]	180	5.80	3.5
Carbon (IM7) [16]	276	5.52	2.0
Carbon (T-1000) [17]	294	6.37	2.2

Other types of fibers may still be able to provide important contributions to COPVs. For instance, in some cases it is required to add a fiberglass overwrap on a COPV to provide abrasion resistance [18]. Also, incorporation of fibers, such as Kevlar or PBO, into composites can help to increase the impact resistance [19,20].

2.2.2 Resins

A large number of options for polymer-based resins are available for the matrix selection. When determining resin systems of interest, it must be ensured that they are suitable for the operating environment. For a matrix to properly distribute load between fibers it should have a strain to failure higher than that of the fiber. This may be easily accommodated by most resins at ambient conditions. However, under cryogenic conditions many resins may become too brittle to properly distribute load [21].

One must also consider how the properties of the resin will affect the manufacturing conditions of the composite. For wet filament winding, the viscosity of

the resin should be 2,000 cps or lower [8]. The low viscosity promotes fiber wetting and reduces the creation of air bubbles. This results in a smoother, denser composite. For prepreg systems, a higher viscosity resin is favorable. The resin pot life is also a major factor in whether or not a resin system will work for wet windings. Although polyurethane systems provide the ductility needed for cryogenic COPVs [2], their pot lives tend to be so short that the resin sets before the part is finished. Whatever the chosen resin system is, the mechanical properties and working parameters should be evaluated prior to the fabrication of a COPV.

2.2.3 Fiber Sizing

Sizing/finish, a chemical agent applied to fibers immediately after their formation, determines how fibers will handle during processing and enhances the fiber/matrix bond. Figure 2.6 illustrates the role of fiber sizing. One may choose to have a sizing specially formulated for a particular resin system, but this is often costly and time consuming. On the other hand, one may choose a more general sizing that is compatible with several systems. However, use of a multicompatible sizing may come with a performance penalty of the end product's mechanical properties. Chapter 3 discusses the reported methods of evaluating the fiber/matrix interface.

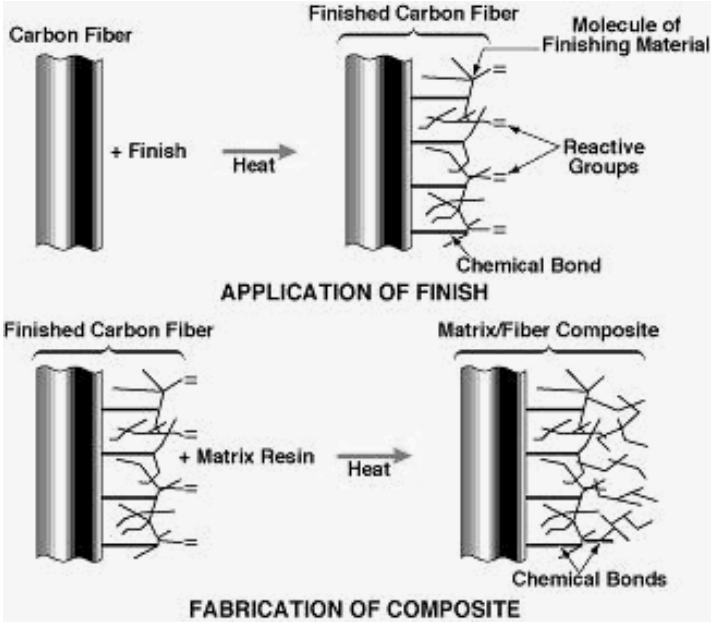

Figure 2.6: Role of fiber sizing/finish [22]

The potential adverse effects of fiber sizing should also be considered. In some studies, the addition of sizing has actually been seen to decrease the strength of uniaxial composites [23]. The sizing can act as a barrier to resin permeability into fiber tows, resulting in low resin content and increased flaws which act as stress concentrations.

CHAPTER 3

EVALUATION OF CONSTITUENT COMPATIBILITY

Once it is decided what fibers and matrix systems are of interest, there exists the question of whether or not the chosen constituents will interact well. Foremost is the ability to transfer the applied loading from fiber to fiber. Additional factors include fiber wettability, the ability of the matrix to saturate the fibers. This is particularly important to the manufacturability of the composite. The full strength of the composite cannot be realized if the matrix material does not properly impregnate the fibers.

To optimize the material selection process for cryogenic COPVs, some evaluation technique is needed to select viable combinations of fiber and matrix. The chosen technique should be easily repeatable so that results taken by various people at various stages in the COPV development are comparable.

3.1 Interfacial Shear Strength (IFSS) Testing

Composites are usually evaluated by means of various standard tensile, flexural, and fatigue tests performed on actual specimens. These tests provide valuable information about the overall properties of the composite, but their results are dependent on factors such as specimen geometry, volume fraction, and fiber aspect ratio. Direct information about the fiber/matrix interface cannot be obtained by such tests.

Instead a more micromechanical technique may be needed. There are four reported methods for evaluating the interface [24]: the single fiber pull-out test, the microbond test, the fragmentation test, and the indentation test.

3.1.1 Single Fiber Pull-Out Test

In the pull-out test a single fiber is embedded in a thin sheet of resin, which is then allowed to cure. The specimen is placed in a tensile test machine with the sheet of resin mounted to a holder and the free fiber end gripped by the load cell. The fiber is then pulled from the resin while recording the load and displacement values. This method is shown in Figure 3.1.

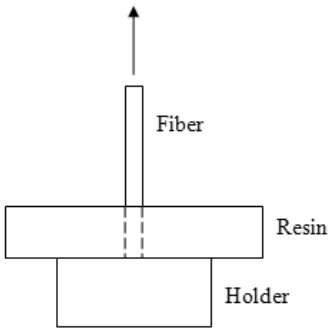

Figure 3.1: Single fiber pull-out test method

To make such pull-out measurements, the embedded fiber length must be small enough such that the fiber does not break before it pulls free. With fibers of small diameter, such as carbon (5-8μm), typically the embedded length of fiber cannot exceed a few tenths of a millimeter [25,26]. The attraction of the resin to the fiber causes a meniscus to form, which causes further difficulty with keeping small embedded lengths.

Being that single carbon fibers are fragile, the difficulty of preparing, handling, and testing such samples limits the success of this method. Some authors have reported limited success with carbon fibers, although no data was reported in the open literature.

3.1.2 Microbond Test

The microbond test is much like the pull-out test, except that instead of embedding a fiber in a sheet of resin, a droplet of resin is placed on the fiber. After curing, the size of the bead is measured to obtain the embedded length. The sample is placed in a tensile testing machine such that the fiber end is gripped by the load cell and the droplet is placed between two knife edges. By restraining the droplet from displacement with the knife edges, load is applied to the fiber/resin interface. The load, displacement, embedded length, and fiber diameter is recorded. Figure 3.2 illustrates this test method.

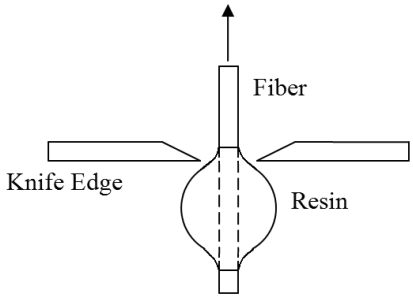

Figure 3.2: Microbond test method

The size of the droplet is crucial to the success of this technique; it determines not only the embedded length but also the symmetry of the droplet, shape of the meniscus produced with the fiber, and the variations in the concentration of hardener within the

droplet. All these factors can influence the value of the IFSS [24]. Like the pull-out test, this method is further complicated by the fragile nature of carbon fibers.

3.1.3 Fragmentation Test

The fragmentation test sample consists of a single fiber encapsulated in a chosen matrix. The sample normally has a dog bone shape with the fiber carefully aligned down the center, as seen in Figure 3.3. The sample is placed in a tensile testing machine, where elongation of the sample results in fiber breakage. The test is typically done under a light microscope or acoustic emission so that the fragmentation process can be observed in place. The fiber breaks into increasingly smaller fragments at locations where the fiber's axial stress reaches its tensile strength. Eventually the fragments will become constant as the fragment length is too short to transfer enough stress into the fiber to cause further breakage. From this critical fiber length the IFSS can be determined.

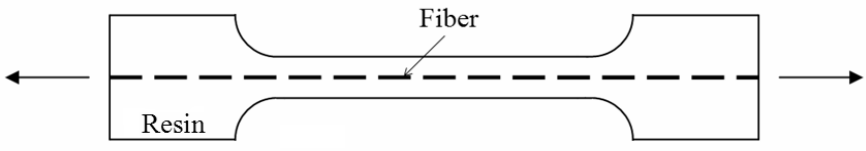

Figure 3.3: Fragmentation test method

An issue with using this method for high-modulus fibers is that they fibrillate on fracture. This makes it difficult to determine the exact fragmentation length [27]. At cryogenic conditions this method may not be feasible due to the matrix becoming brittle. A ratio of about 3:1 of the matrix strain to failure to that of the fiber is necessary for the fragmentation test to work [28]. At cryogenic temperatures, the strain to failure ratio of most polymeric resins compared to carbon fiber is approximately 1:1 [29].

3.1.4 Indentation Test

The indentation test sample is a cross-section of composite that has been carefully polished. A compressive force is applied to an individual selected fiber to produce debonding. The load is applied through an indentor which is smaller than the diameter of the fiber. The IFSS is then derived from the recorded debond load. Figure 3.4 shows the indentation test setup.

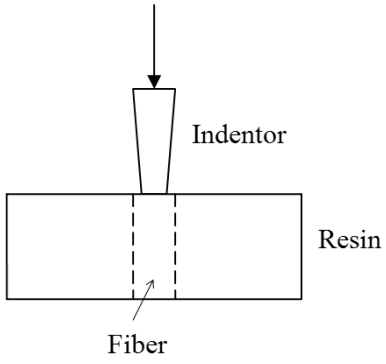

Figure 3.4: Indentation test method

The indentation method is performed on real composites, so it has the advantage of reflecting actual processing conditions. A disadvantage is that to perform this test, specialized equipment is needed. The indentor tip should be smaller than the diameter of the fiber (< 5μm). Imagery capability is also necessary to ensure the indentor is pressed into the center of the fiber. Accuracy of the test can also be affected by fiber geometry and packing conditions. Care must be taken to avoid fiber to fiber contact and resulting friction effects.

3.2 Wettability Testing

Another important consideration in the evaluation of constituent compatibility is the attraction of the resin to the fiber, also known as wettability. Fiber wettability has a strong influence on the interfacial adhesion between fiber and matrix. Incomplete wetting may produce interfacial defects and reduce the IFSS by flaw-induced stress concentrations. Better wetting can also enhance the IFSS by improving the work of adhesion. High surface energy indicates that the fiber contains more polar groups on the surface. Interfacial adhesion can be improved by the strong interaction between resin and the polar groups [30]. A popular method of evaluating wettability is the dynamic contact angle analysis system. Although wettability does not provide insight to the effects of cryogenic temperatures on IFSS, it still seems a useful tool to ensure that strong adhesion exists in the first place.

3.3 Composite Coupon Testing

Macromechanical properties of a composite cannot be easily correlated with interfacial properties measured from the micromechanical tests. They tend to be a complex function of IFSS, fiber volume fraction, and other variables. Another way of looking at fiber/matrix compatibilities would be the use of composite coupon testing. This macromechanical approach would take some factors into account that are missed by micromechanical testing, such as fiber-to-fiber interactions and more realistic manufacturing/curing conditions.

3.3.1 Straight-sided Specimen

The most common composite coupon is one that has been machined from a flat panel of composite material, as described in the ASTM D 3039 standard [31]. The design typically used is the straight-sided specimen with end tabs, shown in Figure 3.5. The tabs are used to create a transition in thickness to reduce the chance of specimen failure in the grip area.

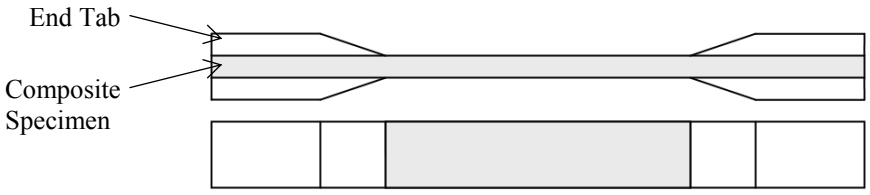

Figure 3.5: Typical composite straight-sided specimen geometry [31]

When testing unidirectional composite materials in the longitudinal direction, special care must be taken to ensure that the loading direction matches the fiber direction. If a 1° mismatch occurs, a reported decrease of as much as 30% in the longitudinal tensile strength could result [5].

3.3.2 NOL Ring Specimen

When selecting the type of test specimen for the experimental characterization of a composite material, one should use a type of specimen that has been made in the same manner as the full-scale, end-product structure [32]. This means that if the end-product structure is a filament wound cylindrical pressure vessel, then the optimal specimen would be a ring or tube taken from a filament wound material. It is extremely difficult, or even impossible, to achieve the same fiber volume fraction, fiber spacing, curing conditions, and other variables of a filament wound article when a straight-sided specimen is used.

Introduced in the late 1960s by the Naval Ordnance Laboratory (NOL), ring-type specimens cut from filament wound tubes became a new option for evaluating composite materials at various temperatures [33]. They are manufactured by filament winding over a mandrel. The composite tube is then removed from the mandrel and cut into the desired ring width. To obtain tensile strength values of the composite, the rings can be tested using the split-D loading device shown in Figure 3.6.

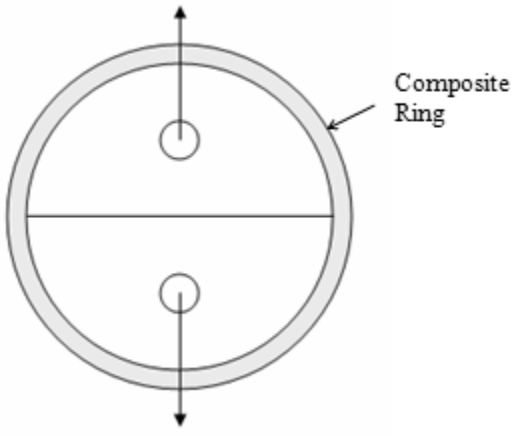

Figure 3.6: NOL ring split-D loading device

NOL rings are not capable of capturing the effects of helical wraps. To avoid cut-fiber effects, the rings are typically composed of hoop wraps only. Results of the method do not reflect true tensile strengths, due to bending moments set up at the plane of separation of the disc halves. However, for comparative purposes, the method is considered most satisfactory [33]. Other methods of testing NOL Rings have been developed to alleviate the bending moment issue, such as internal-pressure loading through use of an inflatable bladder [34]. However, under cryogenic conditions the bladder would likely become brittle and cease to function properly.

3.4 Tank Testing

Although often being cost prohibitive, sometimes it is necessary to build actual COPVs for evaluation. There are some effects that cannot be captured by coupon testing. Additionally, this data is essential to know if results of constituent and composite coupon testing relate well to actual tank performance. Subscale tanks may be used, although scalability of the results is an issue to consider.

CHAPTER 4

EXPERIMENTAL PROCEDURE

The use of COPVs in cryogenic applications, such as fuel storage tanks, requires a strong understanding of how the materials will behave when subjected to the environment. Cryogenic temperatures require the polymer matrix to operate well below the glass transition temperature (T_g). Thus, the performance of a COPV that has been designed for ambient conditions could significantly change when it is subjected to a cryogenic environment. This necessitates the need to understand environmental effects on the mechanical properties of polymeric based composites.

Efforts start with the evaluation of the neat resins at MSU. Initial screening was done at ambient and LN_2 conditions. Following this testing, candidates of interest were further tested in LH_2 at the NASA-MSFC. To gain insight into the effects of fiber sizing, a study was done in which the performance of composites employing three different fiber treatments were compared using NOL ring tests. To assess the compatibility of various fiber/matrix combinations, straight-sided and NOL ring samples were manufactured and tested. Testing of the straight-sided, constant rectangular cross section type sample is the commonly accepted method for determining tensile properties of polymer matrix composite materials. However, following the NOL ring method allows the manufacturing conditions of the test sample to be more comparable to that of an actual

vessel. For this study, both methods were utilized and the results compared. Fabrication and testing of COPVs at the NASA-MSFC provides tank performance data to which small scale constituent and composite testing may be compared. This step is necessary to verify that the test methods used for material screening are meaningful.

4.1 Neat Resin Specimen

A variety of commercial and experimental resins were tested in uniaxial tension to determine their mechanical properties at ambient, LN_2, and LH_2 temperatures. Although it does not include testing at cryogenic conditions, the ASTM D 638 standard [4] was used as a guideline for the test procedure. At LN_2 temperatures, the use of the type IV specimen geometry resulted in stress risers in the transition region which caused premature failure in the grip area. A modified geometry, which provided a more uniform stress transition, was used to alleviate the premature failure [21].

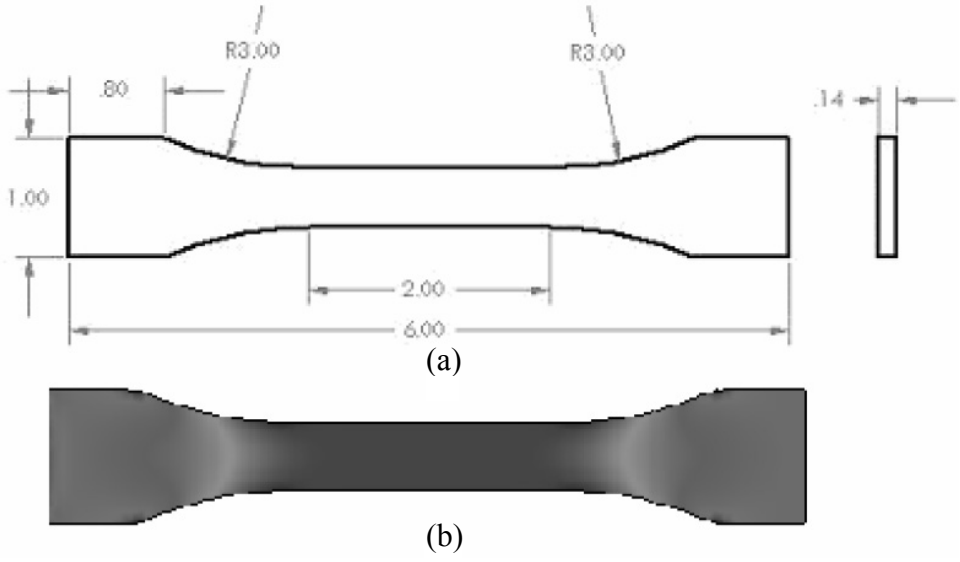

Figure 4.1: (a) Modified dog bone geometry (dimensions are in inches) and (b) results of FEA showing stress distributed over the gage section [21]

Samples were machined from cast sheets of resin. The resins were prepared following manufacturers' recommendations. After thoroughly mixing, the resin was degassed using a vacuum pump. The prepared resin was cast using a three piece aluminum mold and then cured in a BlueM model number EM-9665R1G-MPZ.GOP oven. Table 4.1 shows the curing conditions for the various resin systems presented in this paper. Cured sheets of resin (3.5mm thick) were cut using a band saw into strips (25 mm x 177 mm x 3.5 mm). Using a TensilKut model 10-33 router table with a specialized jig [21], the resin strips were machined into the final dog bone geometry. Attempts were also made to use a mold that directly yields the dog bone samples and eliminates the need for machining. However, there was a tendency for air bubbles to become trapped in the transition region and resulted in premature failure of many of these samples. Thus, the success of this net shape fabrication method was found to be very limited.

Table 4.1: Curing conditions for resin systems

Resin	Curing Cycle	
	Time (hr)	Temperature (°F)
HEI 535 [35]	24	185
EPON 862/W [36]	8	255
EPON 828/L [37]	1	300
CTD 7.1 [38]	8	120
TD 111103 [39]	8	250
Urethane 15-SP [39]	4	160
Urethane 15-55 [39]	6	160
Urethane AK423 [39]	8	160

4.2 Neat Resin Testing

Tests were conducted using an Instron Model 5869 EM load frame equipped with a 50 kN load cell. Prior to testing in LN_2, the samples were dipped in LN_2, to allow thermal contraction, before being loaded into the grips and bolted using a torque of 10 N-m as shown in Figure 4.2a. A MTS Model 634.11E-21 extensometer, also shown in Figure 4.2a, was attached using rubber bands. The instrumented sample was loaded into the cryostat shown in Figure 4.2b. With the load frame operating in load control mode, the cryostat was filled with LN_2 and allowed to reach thermal equilibrium (approximately 10 minutes). The load frame was then changed to displacement control and the test conducted at a constant crosshead speed of 0.127 cm/min until failure was observed as indicated by a load drop of more than 60%.

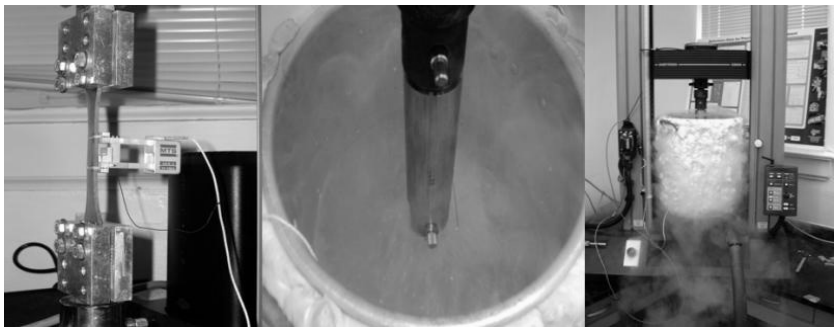

(a) (b) (c)

Figure 4.2: Overview of LN_2 temperature tension testing facility at MSU. (a) MTS extensometer attached to specimen mounted in grips, (b) interior of cryostat, and (c) cryostat mounted on Instron load frame

For ambient temperature testing, the specimens were loaded in wedge action grips and instrumented with an Instron Model 2630-115 extensometer. All tests were run in displacement control at a constant crosshead speed of 0.127 cm/min to be consistent with the LN_2 temperature tests. Because of the variation in ambient properties, the crosshead speed of 0.127 cm/min does not conform in all cases to the recommended rates of the ASTM D638 standard. To address possible strain rate affects on the properties, additional representative samples were run at crosshead velocities in compliance with ASTM D638.

Representative samples were also tested at LH_2 temperatures using the facilities at the NASA-MSFC. A MTS Model 810 servo-hydraulic load frame with a 100 kN capacity load cell was used to conduct the tests. The load frame utilized a Teststar IIM controller hub. These tests were run at a constant crosshead velocity of 0.127 cm/min. The specimens were held submersed in the LH_2 for 5 minutes to reach thermal equilibrium prior to initiation of the test. Specimen temperature was verified by thermocouples attached to the test fixture.

4.3 Straight-sided Specimen

After identifying constituents of interest, various combinations of fiber and matrix were produced to evaluate the performance of the resulting composites. Panels were manufactured at Hypercomp Engineering, Inc. [40]. Using an Entec PW65H-120-4-2S filament winding system, the composites were wet-wound onto a rectangular mandrel. Peel ply was added to locations of the composite that corresponded to the grip areas of the final specimens. After curing, the composite was cut from the mandrel resulting in

two flat composite plates. The flat plates were then cut into tensile specimens using a wet tile saw with a diamond abrasive blade. Lay-up parameters and machining were adjusted to produce a 0° unidirectional tensile specimen geometry as recommended by ASTM D 3039 [31] (15 mm x 250 mm x 1.0 mm).

4.4 Straight-sided Specimen Testing

Tests were conducted using an Instron Model 5869 EM load frame equipped with a 50 kN load cell. The most difficult issue with the straight-sided specimen testing under cryogenic conditions was the gripping of the samples, mostly due to thermal contraction. Use of bonded tabs always resulted in specimen slippage, and mechanical wedge action grips would cease under cryogenic temperatures. The solution was the use of bolted grips, shown in Figure 4.3. 80 grit emory cloth was first bonded to each of the grip faces using Hysol EA9394 structural adhesive. Hysol was also added between the sample and the emory cloth. After bolting the sample into the grips using a torque of 20 N-m, the adhesive was allowed to cure. Prior to testing, the samples were dipped in LN_2 to allow thermal contraction. The bolts were then retightened to 20 N-m and the sample was loaded into the cryostat. To obtain the modulus of elasticity, a MTS Model 634.11E-21 extensometer was attached to the sample. With the load frame operating in load control mode, the cryostat was filled with LN_2 and allowed to reach thermal equilibrium (approximately 10 minutes). The load frame was then changed to displacement control and the test conducted at a constant crosshead speed of 0.127 cm/min until failure was observed as indicated by a load drop of more than 60%. Grips were scraped clean after testing and the preparation process was repeated for each sample.

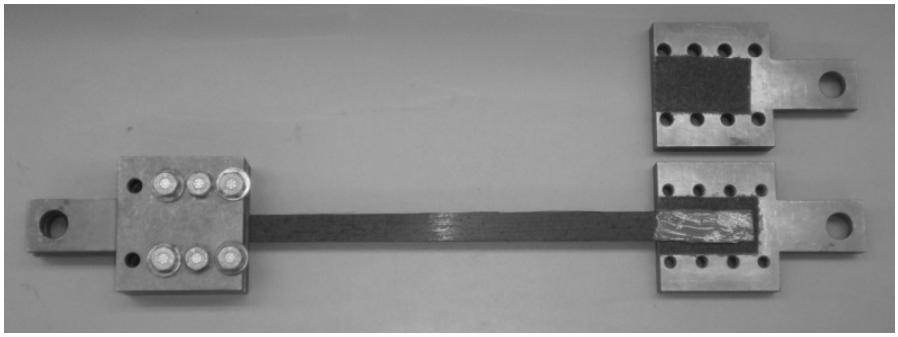

Figure 4.3: Straight-sided specimen in bolted grips

For ambient temperature testing, the specimens were loaded in wedge action grips and instrumented with an Instron Model 2630-115 extensometer. All tests were run in displacement control at a constant crosshead speed of 0.127 cm/min to be consistent with the LN_2 temperature tests.

4.5 NOL Ring Specimen

NOL Ring specimens were wound at the NASA-MSFC using an Entec 5K48W-180-4 filament winding system. 102 cm long by 15 cm diameter composite tubes were fabricated using a polished aluminum tube as a mandrel. Before winding, the mandrel was coated with Frekote 700NC mold release. For urethane based resins a mold wax was used instead. The composite samples were wet wound using a tension of 22.24 $\pm$ 0.004 N, controlled by precise fiber tensioners from Helman Engineering, Inc. Five hoop wraps were made around the mandrel with a single tow, [+88°/-88°/+88°/-88°/+88°], which resulted in an average composite thickness of 0.06 cm. The composite tubes were vacuum bagged to minimize defects, and cured in a fashion optimal for the specific resin being used. After curing, the composite tubes were

removed from the mandrel and cut into rings 2.5 cm and 0.9 cm wide. The 2.5 cm wide rings were used in the NOL ring testing at the NASA-MSFC. Due to load frame limitations, 0.9 cm width rings were the maximum that could be tested at MSU. A comparison is presented in Chapter 5 to evaluate ring width effects.

4.6 NOL Ring Specimen Testing

Rings of 2.5 cm width were tested at the NASA-MSFC using a MTS Model 810 servo-hydraulic load frame with a 100 kN capacity load cell. The load frame utilized a Teststar IIM controller hub. Tests were conducted using the split-D loading device at ambient (298 K), LN_2 (77 K), and LH_2 (20 K). Rings of 0.9 cm width were tested at MSU using Instron Model 5869 EM load frame equipped with a 50 kN load cell. Figure 4.4 shows a close up of the self-aligning split disk fixture that applies tensile stress to the rings. After loading into the test frame, the specimens were submersed in the liquid and held for 5 minutes to reach thermal equilibrium. Tests were conducted at a loading rate of 0.25 cm/min. In addition to the test parameters outlined in the NOL documents [33], an ASTM standard exists for similar testing at ambient conditions [41]. An apparent hoop tensile strength (σ) was calculated from the maximum load using:

$$\sigma = \frac{P}{2A} \tag{4-1}$$

where:

P = maximum load

A = cross sectional area (hoop width × ring thickness)

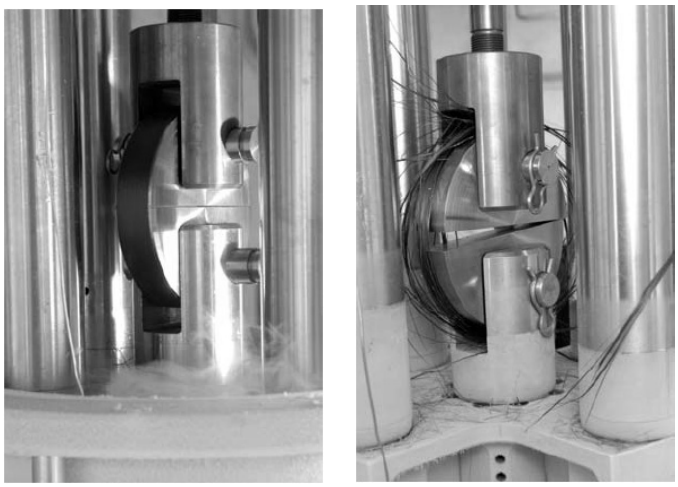

(a) (b)

Figure 4.4: Close up of split-D test fixture. (a) Prior to submersion in LN_2 and (b) after completion of test

4.7 COPV Fabrication

After reviewing the results of constituent and composite coupon testing, fiber/resin combinations of interest were then used to build COPV test specimens. Tank manufacturing and testing was done at the the NASA-MSFC. To minimize concerns of resin microcracking and permeability, a liner is often used in the COPV construction. An AA 6061 dual port 7.5 liter seamless liner supplied by SAMTECH Intl., Inc. [42] was the liner and also served as the mandrel. Before winding, the liner was coated with mold release to discourage bonding with the overwrap. The COPVs were wet wound using an Entec 5K48W-180-4 filament winding system, with fiber tension controlled by a tensioner creel from Helman Engineering, Inc. The processing parameters were precisely replicated such that an accurate comparison between material systems could be made.

Parameters include: number of fiber tows, bandwidth of the combined tows, fiber tension, wind angles, and layer sequence. The winding sequence consisted of 3 hoop, [+88°/-88°/+88°], and 1 helical, [±18°], wrap. The manufacturer's cure cycle recommendation for each resin system was followed.

4.8 COPV Burst Testing

Sample vessels were burst under ambient (298 K) and LN_2 (77 K) conditions. Ambient tests were conducted using a hydrostatic burst pump. LN_2 tests were performed using the NASA's LN_2 burst test facilities, shown in Figure 4.5. In addition to filling the test vessel with LN_2, the vessel was also submerged in LN_2 to ensure uniform temperature of the material. The rise rate for the pressurization was approximately 0.6-0.7 MPa/sec. Use of a cascade vessel ensured that no gaseous nitrogen remained in the vessel, resulting in a strictly hydraulic burst mode.

To compare results of the COPV burst testing, the delivered fiber strength (DFS) of each vessel is calculated. Manufacturer's fiber strength data comes from uniaxial tensile measurements. However, in application a decrease in fiber performance is seen due to factors such as multiaxial loading. Delivered fiber strength refers to a ratio of demonstrated fiber strength to manufacturer's specified fiber strength. Using finite element analysis (FEA), Hypercomp Engineering, Inc. used the burst data and composite lay-up parameters to calculate the DFS for each vessel [40]. The calculation also takes into account the contribution of the metal liner.

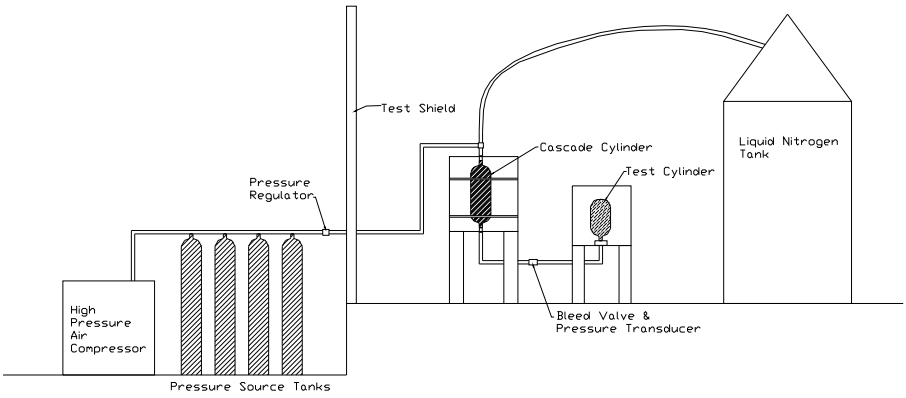

(a)

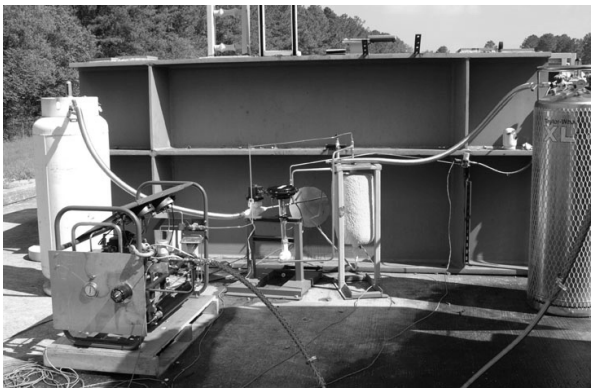

(b)

Figure 4.5: (a) Schematic of LN_2 burst test and (b) the NASA's LN_2 burst facility

CHAPTER 5

RESULTS AND DISCUSSION

Using the methodology outlined in the previous chapter, data was gathered for a variety of constituents and composite systems. The creation of this database of material properties, especially at cryogenic temperatures, is one of the significant achievements of this research project. It is often possible to find ambient properties, and sometimes even properties at elevated temperatures. However, data at cryogenic conditions either does not exist or is not found in open literature. Using the newly established database, this chapter will attempt to correlate constituent and composite properties with COPV performance. Results are shown in bar charts for comparison purposes. Material properties in table form are presented in the appendix.

5.1 Neat Resin Testing Results

Figures 5.1 through 5.3 provide a comparison of the ambient (298 K), LN_2 (77 K), and LH_2 (20 K) temperature properties of various resin systems, two of which (15-SP and 15-55) are urethane based while the others are epoxy based. Other resins systems were tested during the study, but are not presented due to poor performance. For a matrix to properly distribute load between fibers it should have a elongation to failure slightly higher than that of the fiber. Considering the typical 2% elongation to failure of carbon fibers, the resins tested were down selected to those shown as suitable candidates

for use at cryogenic temperatures. Strain rate sensitivity was evaluated for the EPON 862/W and Urethane 15-55 systems. The properties using the ASTM D 638 specified crosshead velocity were found to be similar to those using the 0.127 cm/min crosshead velocity.

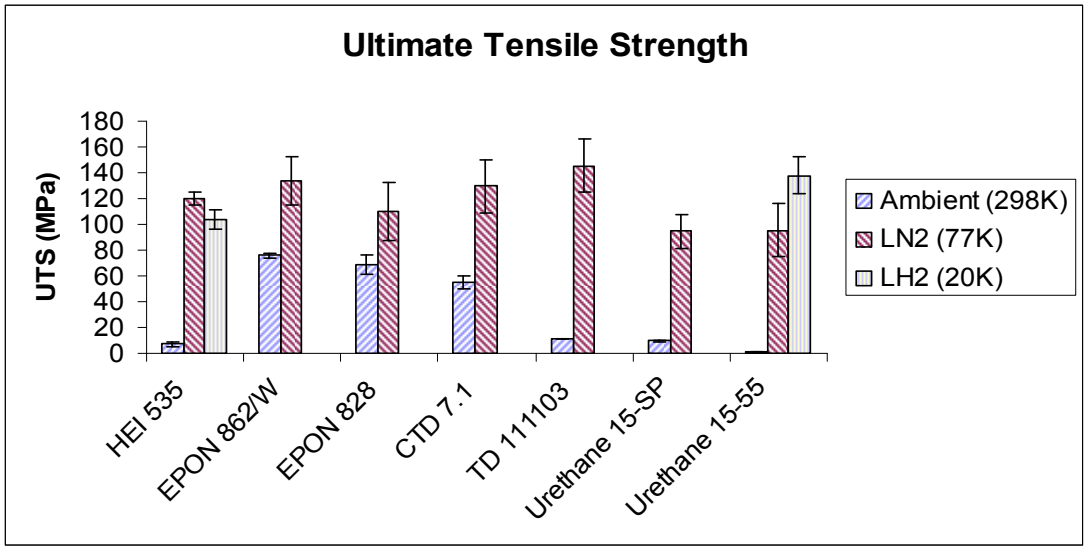

Figure 5.1: Ultimate tensile strength of resins tested at ambient, LN_2, and LH_2

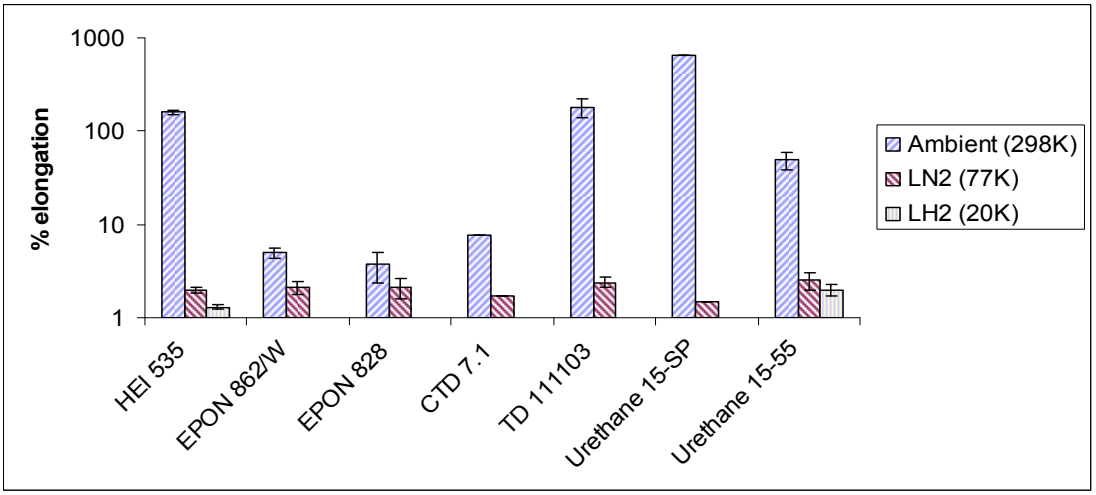

Figure 5.2: Elongation to failure of resins tested at ambient, LN_2, and LH_2

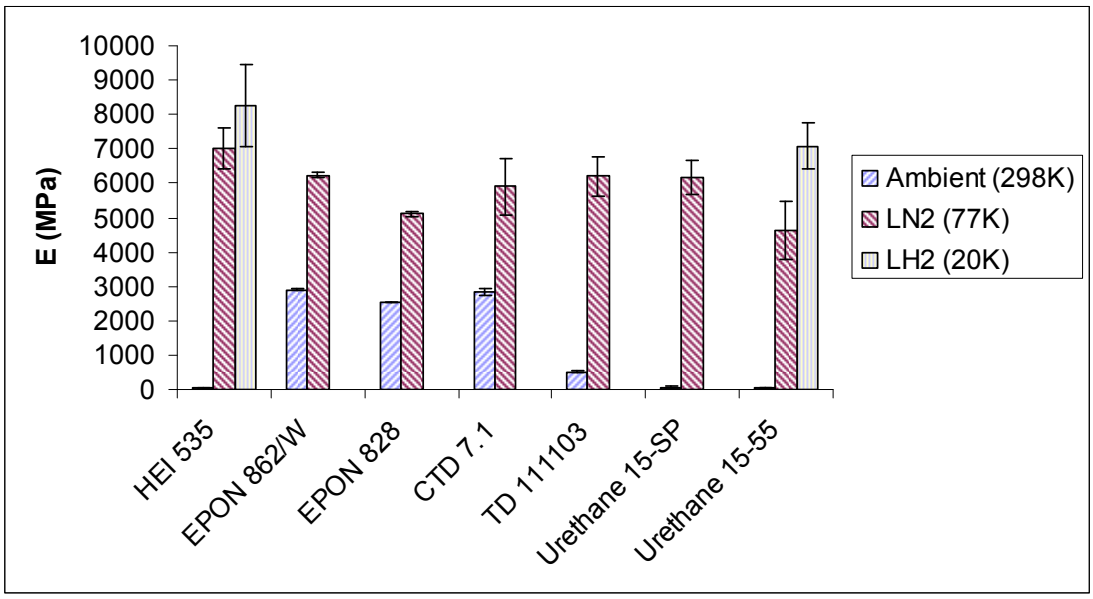

Figure 5.3: Modulus of elasticity of resins tested at ambient, LN_2, and LH_2

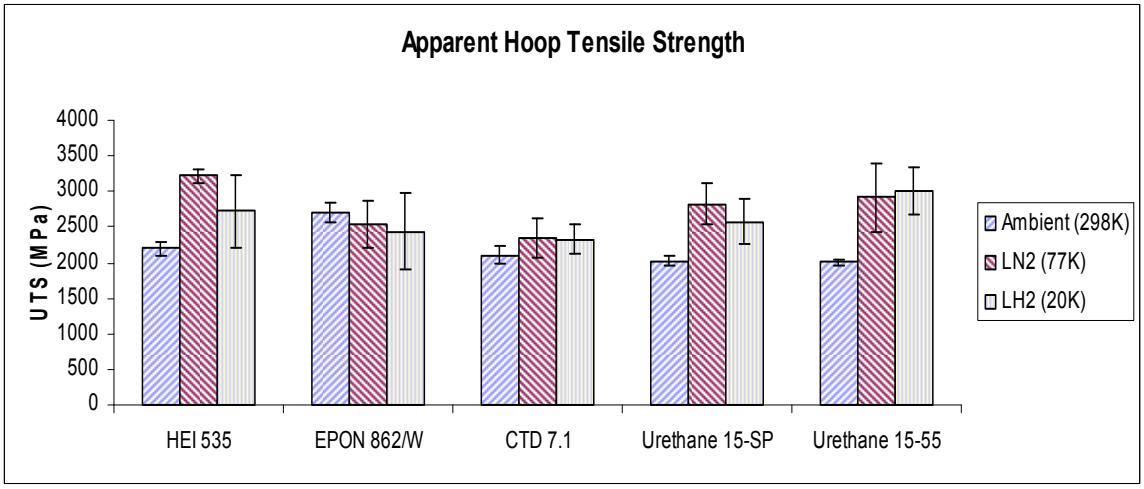

Figure 5.4: Strength of 2.5 cm wide NOL rings with various resins and IM7 fiber [43]

To evaluate the behavior of resin/fiber combinations at cryogenic conditions, composite samples were also tested. Figure 5.4 summarizes the apparent hoop tensile strength of some composites rings made using the various resin systems and the IM7

fiber. When comparing the LN_2 performance of the composites to the properties of the resins at LN_2 temperature, no distinct relationship is observed. However, when considering the difference between the resin modulus at ambient versus LN_2 temperatures, it appears that the better performing composites are those that use "gummy", or less stiff resins, as reflected by an elastic modulus of less than 35 MPa. Due to differences in coefficient of thermal expansion between the fiber and matrix, thermally induced stresses are incurred during chill down. Perhaps the lower stiffness resins are better able to accommodate the thermally induced stresses, resulting in improved survivability of the composite.

5.2 Fiber Sizing Affect on UTS

During the evaluation of many fiber/resin combinations, one aspect that sometimes tends to be overlooked is the fiber sizing. For the most part, it is just assumed that an adequate bond exists. However, if the sizing is not compatible the matrix may not bond properly to the fiber resulting in poor load transfer and reduced mechanical properties. One attempt to address this concern was the manufacture and testing of NOL rings in which the fiber sizing was varied. Three variations of IM7 carbon fiber were used: unsized, sizing compatible with Epon 828 base resin, and sizing compatible with Dow 755 base resin. Rings were constructed using both an epoxy resin (HEI 535 [35]) and an urethane resin (AK423 [39]).

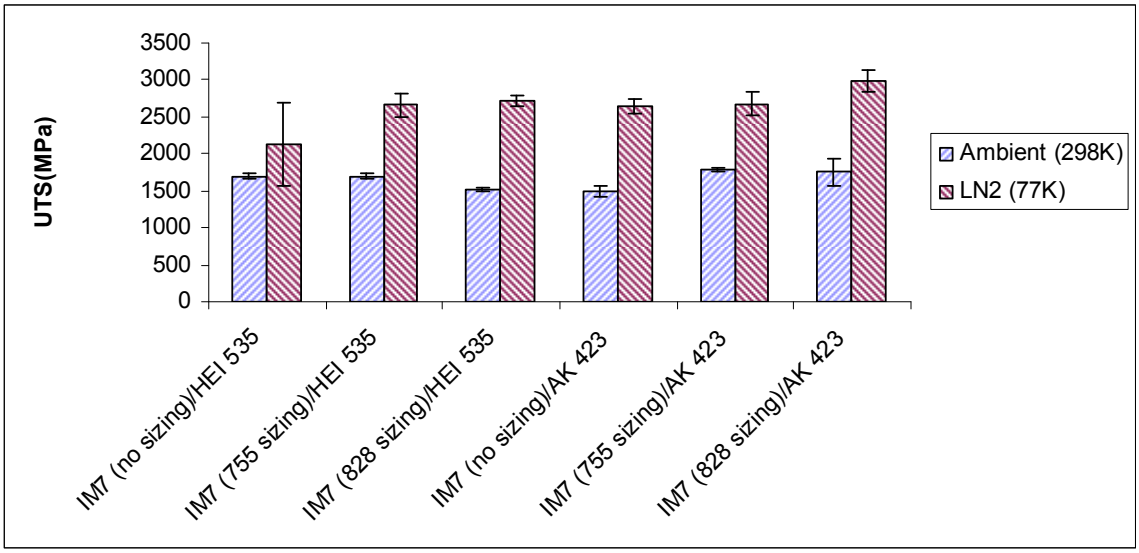

Figure 5.5: Strength of 2.5 cm wide NOL rings with various resins and IM7 fiber with various sizings

Figure 5.5 shows the apparent hoop tensile strength of the NOL rings tested. When looking at the data, no distinguishable pattern is seen. In the composites in which no sizing is used, the tensile strength is not greatly reduced. This suggests that in the case of unidirectional continuous fiber composites, fiber sizing does not significantly affect the composite's ultimate tensile strength. In discussion with Adherent Technologies, Inc. [44], the company which supplied the specialty sized fibers, it was agreed that uniaxial tension really does not test the sizing very much. Instead, the sizing comes more into play with off-axis loads and in composite durability.

In the straight-sided and NOL ring composite tensile tests, the fibers are close to uniaxial (± 2°). The results of this testing are reassuring in the sense that some mismatch in sizing/matrix compatibility should not significantly affect the results of the composite tests. Instead, the composite's tensile performance will be a reflection of the fiber and

matrix properties as well as the composite's fiber volume fraction. However, the effect of fiber sizing on fiber wettability and composite durability may still be something to consider in the future.

5.3 NOL Ring Width Affect on UTS

To allow NOL Ring testing at MSU, ring width had to be reduced to 0.9 cm such that the specimens would fail within the capabilities of the load frame. To evaluate the effect of the reduced width on ring performance, Figure 5.6 compares ambient and LN_2 UTS results for both widths. Data for the 2.5 cm wide T-1000/Epon 828/W rings was not available, so the comparison was done for T-1000/HEI 535. The data shows that the narrower ring can be used without a significant change in test results.

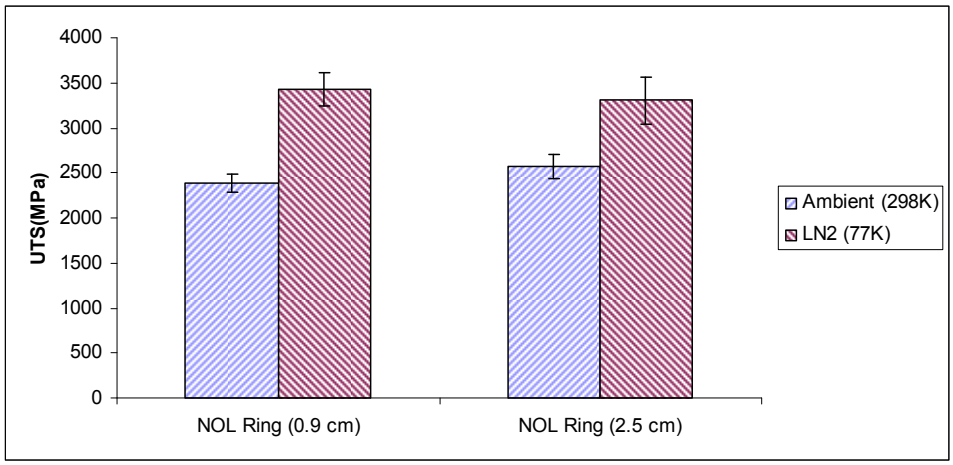

Figure 5.6: T-1000/HEI 535 composite strength comparison for 0.9 cm and 2.5 cm wide NOL rings

5.4 NOL Ring and Straight-sided Comparison

NOL ring and straight-sided specimens were tested and compared for a composite constructed of T-1000 carbon fiber and Epon 828 resin. The goal of this testing was to determine which of the two was the most accurate and repeatable method. Because fiber volume fraction varied between the two specimen types, delivered fiber strength was used as the comparison. As an additional check, following the rule of mixtures, a predicted UTS was calculated using:

$$\sigma = \sigma_f \cdot V_f + \sigma_m \cdot V_m \tag{5-1}$$

where:

σ_f = ultimate tensile strength of fiber

σ_m = ultimate tensile strength of matrix

V_f = fiber volume fraction

V_m = matrix volume fraction

Figure 5.7 shows the results of the composite testing at ambient and LN_2 temperatures. Predicted composite UTS values at ambient and LN_2 temperatures were calculated using corresponding fiber [13] and resin strength values measured at ambient and LN_2 temperatures. Predicted values varied between specimen types due to differences in fiber volume fraction. Comparing actual UTS to predicted UTS at ambient temperature, a reduction of 38% for the NOL ring and 43% for the straight-sided specimen is observed. Considering the ±2° fiber orientation in the specimens along with

reports that even 1° of fiber deviation from the loading axis can reduce the strength by as much as 30% [5], some difference between predicted and actual UTS is expected. In addition to specimen fiber misalignment, factors such as stress concentrations due to gripping and composite flaws can significantly reduce the measured values.

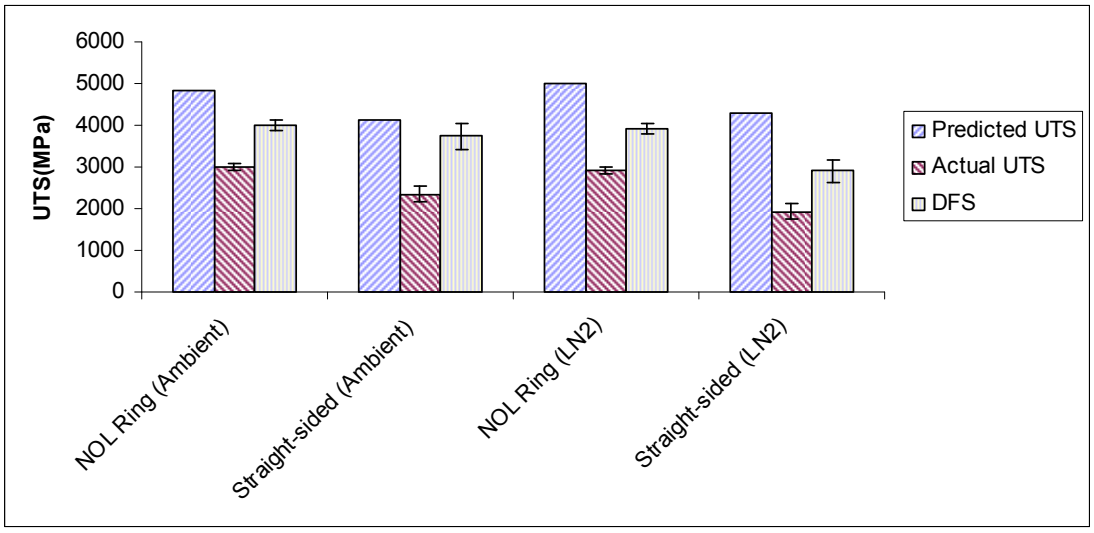

Figure 5.7: T-1000/Epon 828/W composite strength comparison for 0.9 cm wide NOL ring and straight-sided specimens

Comparing the composite test methods it seems that the NOL ring method is the better of the two. Higher DFS values were obtained and the results were more consistent, as reflected by a lower standard deviation. Specimen manufacturing, preparation, and testing was also much easier and repeatable for the NOL rings. Additionally, the NOL rings have the added benefit that the specimens are manufactured in a method almost identical to the hoop wrapped construction of the COPVs.

5.5 NOL Ring and COPV Comparison

After the selection of a preferred test method, the question arises of how well the obtained material performance compares to the performance of an actual component. To help answer this question, materials that have shown promise in early mechanical evaluations are used to build COPVs for burst testing. Figure 5.8 shows a comparison of delivered fiber strengths for various resin systems using IM7 carbon fiber for both NOL ring and COPV burst tests performed at the NASA-MSFC. Although data is limited, the trend for most composite systems compares well between the two test methods. This proves that the NOL ring test method is able to provide a statistically valid, low-cost method for evaluating potential cryogenic COPV materials.

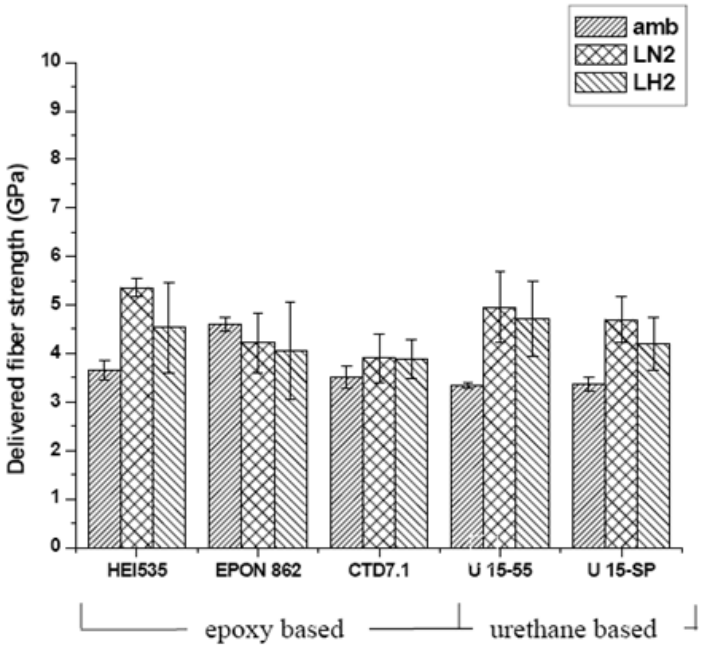

(a) NOL Ring Test Data

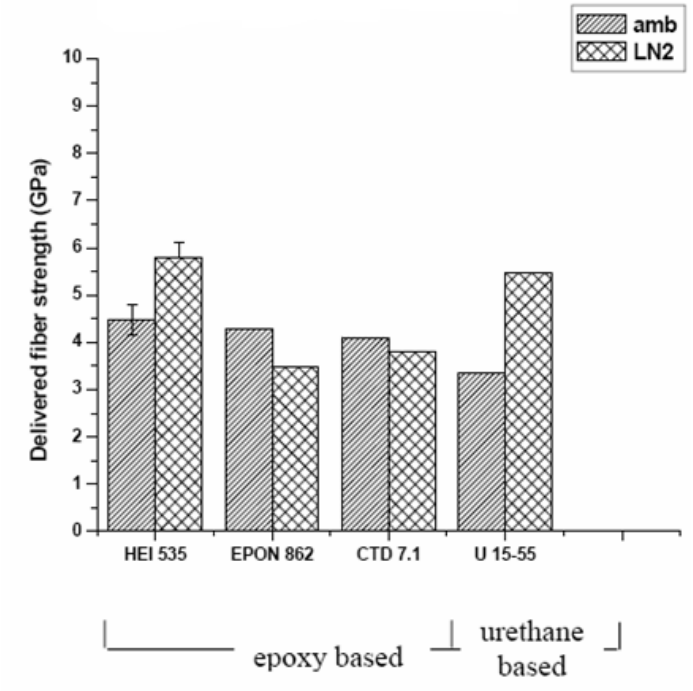

(b) COPV Burst Data

Figure 5.8: Delivered fiber strength for various resin systems with IM7 fiber based on (a) 2.5 cm wide NOL ring tests and (b) COPV burst tests [2]

CHAPTER 6

CONCLUSIONS AND FUTURE WORK

As the field of polymeric composites continues to grow, and the number of available resins and fibers increases, the ability to effectively evaluate composite performance is essential. The chosen method to do so must not only be repeatable among other researchers and laboratories, but should also correlate well with the intended component's performance. The effort of this project is to find such a method and to use it to optimize the material selection process for the design of cryogenic composite overwrapped pressure vessels. Another major intent of the project is to build a much needed database of mechanical properties of composite constituents at cryogenic temperatures.

Investigation into the possible use of micromechanical techniques to evaluate the interfacial shear strength of the fiber/matrix bond in composite materials found them not to be a preferable method. The results of these techniques are very procedure dependent and data scatter between laboratories can be high [24]. The development of standard procedures is needed to improve the validity of such a method. The added difficulty of testing at cryogenic temperatures also limits or prevents the success of the techniques.

The testing of neat resin specimens is proving to be useful. Based on the obtained data, it appears that resins with a LN_2 elongation to failure greater than 2% and with an ambient elastic modulus less than 35 MPa are suitable candidates. If a resin is too brittle and falls outside of these criteria, then it can be dismissed such that future time and resources are not spent on composite testing. Continued resin testing is needed to evaluate other available systems and to improve the statistical validity of the database.

Results of the study on affects of fiber sizing did not show the UTS of unidirectional composites to be significantly influenced. Instead, sizing plays more of a role in off-axis loading and composite durability. While a goal of fiber sizing is to improve composite strength, it can also be responsible for reduced performance. Cases have been seen in which fiber sizing inhibits resin penetration into fiber tows [23]. This can result in low resin content and stress concentrations due to defects. Future testing may include fiber wettability and the affect of sizing on composite durability.

Comparison of the NOL ring test method to the more conventional straight-sided specimen shows that the NOL rings provide better, more consistent results. Higher composite strengths and less data scatter was seen. Repeatability of specimen manufacturing, preparation, and testing, as well as a similarity in fabrication to that of COPVs, demonstrates an advantage to the method. The similarity of NOL ring results to burst performance of actual COPVs also proves the value of the method. Little difference was found in varying the width of the ring specimen, especially at LN_2 temperatures.

With continued testing of constituents, composite coupons, and COPVs, the statistical validity of the gathered data will grow and trends may more clearly emerge. Future areas of interest also include effects of irradiation, thermal and mechanical cyclic degradation, and composite durability.

REFERENCES

[1] "Diagram of Saturn V Third Stage (S-IV B)," *NASA History Division*, 2 March 2008, <http://www.history.nasa.org/MHR-5/Images/fig326.jpg>.

[2] DeLay, T.K., Patterson, J., Noorda, J., Schneider, J.A., June 2007, "Development of Cryogenic Composite Over-Wrapped Pressure Vessels (COPVs)," *SAMPE 52nd International Symposiu*m, Baltimore, MD.

[3] 2003, *Annual Book of ASTM Standards*, Vol 15.03: Space Simulation; Aerospace and Aircraft; Composite Materials.

[4] ASTM D 638, *Standard Test Method for Tensile Properties of Plastics* (1991).

[5] United States. 17 June 2002, *Department of Defense MIL-HDBK-17-1F* Composite Materials Handbook: Volume 1. Polymer Matrix Composites Guidelines for Characterization of Structural Materials.

[6] Hodge, A.J., August 2001, "Evaluation of Microcracking in Two Carbon-Fiber/Epoxy-Matrix Composite Cryogenic Tanks," *NASA/TM-2001-211194*.

[7] Jones, R.M., 1999, *Mechanics of Composite Materials*, 2nd ed., Taylor & Francis, Philadelphia.

[8] Peters, S.T., Humphrey, W.D., Foral, R.F., 1991, *Filament Winding Composite Structure Fabrication*, 2nd ed., Society for the Advancement of Material And Process Engineering, California.

[9] Barbero, E.J., 1999, *Introduction to Composite Materials Design*, Taylor & Francis, New York.

[10] "Filament Winding Process Schematic," *PolymerProcessing.com*, 13 February 2008, <http://www.polymerprocessing.com/operations/filwind/index.html>.

[11] Mallick, P.K., 1993, *Fiber Reinforced Composites*, Marcel Dekker, Inc., New York.

[12] Hanson, M.P., February 1968, "Glass-, Boron-, and Graphite-Filament-Wound Resin Composites and Liners for Cryogenic Pressure Vessels," *NASA/TN D-4412*.

[13] Hastings, W.C., Schneider, J.A., October 2007, "Cryogenic Temperature Effects on the Mechanical Properties of Carbon and Synthetic Fibers," *SAMPE Fall Technical Conference 2007*, Cincinnati, OH.

[14] "Kevlar Aramid Fiber Technical Guide," *DuPont*, 3 March 2008, <http://www2.dupont.com/Kevlar/en_US/assets/downloads/KEVLAR_Technical_Guide.pdf>.

[15] "Zylon (PBO fiber) Technical Information (2005)," *Toyobo*, 3 March 2008, < http://www.toyobo.co.jp/e/seihin/kc/pbo/Technical_Information_2005.pdf>.

[16] "HexTow IM7 (5000) Carbon Fiber Product Data," *Hexcel*, 3 March 2008, < http://www.hexcel.com/NR/rdonlyres/BD219725-D46D-4884-A3B3-AFC86020EFDA/0/HexTow_IM7_5000.pdf>.

[17] "T1000G Technical Data Sheet No. CFA-008," *TorayCA*, 3 March 2008, < http://www.torayusa.com/cfa/pdfs/T1000GDataSheet.pdf>.

[18] March 2007, "Basic Requirements for Fully Wrapped Carbon-Fiber Reinforced Aluminum Lined Cylinders (DOT-CFFC)," *Department of Transportation*.

[19] Noorda, J., Patterson, J., Fronk, T., Swenson, D., DeLay, T., June 2007, "Cryogenic Damage Tolerance Effect on Composite Materials," *52nd International SAMPE Symposiu*m, Baltimore, MD.

[20] Kim, J.K., 1998, "Methods for Improving Impact Damage Resistance of CFRPs," *Key Engineering Materials*, v 141-143, pp. 149-168.

[21] Jackson, J.R., December 2005, "Mechanical testing and evaluation of epoxy resins at cryogenic temperatures," MS Thesis, Mississippi State University.

[22] "Carbon Fiber Finishes/Sizings," *Adherent Technologies, Inc.,* 28 February 2008, <http://www.adherenttech.com/carbon_fiber_finishes.htm>.

[23] Cagliostro, D.E., May 1988, "Effect of Sizing on Composite Properties for Materials Used in the Shuttle Filament Wound Case," *Polymer Engineering and Science*, v 28, pp. 562-567.

[24] Pitkethly, M.J., et al., 1993, "A Round-Robin Programme on Interfacial Test Methods," *Composites Science and Technology*, v 48, pp. 205-214.

[25] Miller, B., Muri, P., Rebenfeld, L., 1987, "A Microbond Method for Determination of the Shear Strength of a Fiber/Resin Interface," *Composites Science and Technology*, v 28, pp. 17-32.

[26] Piggott, M.R., 1987, "Debonding and Friction at Fibre-Polymer Interfaces. I: Criteria for Failure and Sliding," *Composites Science and Technology*, v 30, pp. 295-306.

[27] Li, Z.F., Grubb, D.T., 1994, "Single-fibre polymer composites," *Journal of Materials Science*, v 29, pp. 189-202.

[28] Favre, J.P., Jacques, D., 1990, "Stress transfer by shear in carbon fibre model composites Part 1: Results of single-fibre fragmentation tests with thermosetting resins," *Journal of Materials Science*, v 25, pp. 1373-1380.

[29] Dyess, M.V., Hastings, W.C., Schneider, J.A., DeLay, T.K., June 2007, "A Systematic Approach to Cryogenic COPV Design," *52nd International SAMPE Symposiu*m, Baltimore, MD.

[30] Chen, P., et al., 2006, "Influence of fiber wettability on the interfacial adhesion of continuous fiber-reinforced PPESK composite," *Journal of Applied Polymer Science*, v 102, pp. 2544-2551.

[31] ASTM D 3039, *Standard Test Method for Tensile Properties of Polymer Matrix Materials* (2000).

[32] Bert, C.W., 1974, "Static Testing Techniques for Filament-Wound Composite Materials," *Composites*, v 5, pp. 20-26.

[33] 1964, "NOL Ring Test Methods," *Naval Ordnance Lab*, White Oak, MD, NOLTR 64-156.

[34] Cohen, D., Toombes, Y.T., Johnson, A.K., Hansen, M.F., 1995, "Pressurized Ring Test for Composite Pressure Vessel Hoop Strength and Stiffness Evaluation," *Journal of Composites Technology & Research*, v 17, pp. 331-340.

[35] "HEI 535 Proprietary Epoxy Resin" *Hypercomp Engineering, Inc.*, 3 March 2008, <http://www.hypercompeng.com>.

[36] "Epon 862/W Product Bulletin," *Resolution Performance Products*, 3 March 2008, <http://www.resins.com/resins/am/pdf/SC1183.pdf>.

[37] "Epon 828 Product Bulletin," *Resolution Performance Products*, 3 March 2008, <http://www.resins.com/resins/am/pdf/SC1547.pdf>.

[38] "CTD 7.1 Epoxy Resin," *Composite Technology Development, Inc.*, 3 March 2008, <http://www.ctd-materials.com/index.htm>.

[39] "Experimental resin system," *Tom DeLay*, Materials, Processes, and Manufacturing Department, NASA Marshall Space Flight Center.

[40] 2007, Contribution performed during work on NASA-STTR Phase I Contract #NNM05AA61C and NASA-SBIR Phase II Contract # NNM05AA45C, *Hypercomp Engineering, Inc.*

[41] ASTM D 2290, *Standard Test Method for Apparent Hoop Tensile Strength of Plastic or Reinforced Plastic Pipe by Split Disk Method* (2000).

[42] "AA 6061 seamless liner supplier," *SAMTECH Intl., Inc.*, 3 March 2008, <http://www.samtech.co.jp/e/sii/index.html>.

[43] Schneider, J.A., Gargis, M., DeLay, T.K., June 2007, "Apparent Hoop Tensile Strength of Fiber Reinforced Composites at LN_2 Temperatures," *52nd International SAMPE Symposiu*m, Baltimore, MD.

[44] Allred, R., CEO Adherent Technologies, Inc., Private Conversation, Fall 2007.

APPENDIX

MEASURED MATERIAL PROPERTY VALUES

Table A.1: Resin properties at ambient temperature tested at 0.127 cm/min crosshead velocity

Resin ID	UTS (MPa)	N	E (MPa)	N	$\varepsilon_{failure}$ (%)	N
HEI 535 [35]	6.9 ± 1.4	4	28 ± 7	4	161 ± 9	1
EPON 862/W [36]	75.8 ± 2.1	4	2903 ± 41	4	5.0 ± 0.6	4
EPON 828/L [37]	68.9 ± 7.6	4	2537 ± 21	2	3.7 ± 1.3	4
CTD 7.1 [38]	55.2 ± 4.8	3	2848 ± 110	3	7.6	1
TD 111103 [39]	11.0 ± 0.0	3	503 ± 28	3	181 ± 40	3
Urethane 15-SP [39]	9.7 ± 0.7	3	62 ± 14	3	660*	3
Urethane 15-55 [39]	1.4 ± 0.3	3	3.8 ± 0.1	3	49 ± 11	3

N = number of samples tested.
* = intentionally terminated.

Table A.2: Resin properties at ambient temperature tested at varying crosshead velocities in accordance with ASTM D 638

Resin ID	UTS (MPa)	N	E (MPa)	N	$\varepsilon_{failure}$ (%)	N
EPON 862/W[1] [36]	71.7 ± 8.3	2	2820 ± 7	2	4.4 ± 1.5	2
Urethane 15-55[2] [39]	2.1 ± 0.1	2	3.8 ± 0.1	2	71 ± 4	2

N = number of samples tested.
[1] = crosshead velocity of 0.5 cm/min
[2] = crosshead velocity of 5 cm/min

Table A.3: Resin properties at LN_2 temperature

Resin ID	UTS (MPa)	N	E (MPa)	N	$\varepsilon_{failure}$ (%)	N
HEI 535 [35]	120.0 ± 4.6	3	7005 ± 593	3	2.0 ± 0.14	3
EPON 862/W [36]	133.8 ± 18.5	5	6240 ± 90	5	2.1 ± 0.32	4
EPON 828/L [37]	110.3 ± 22.3	4	5102 ± 90	3	2.1 ± 0.51	4
CTD 7.1 [38]	129.6 ± 20.7	2	5916 ± 820	4	1.7	1
TD 111103 [39]	145.5 ± 20.2	6	6205 ± 565	6	2.4 ± 0.30	6
Urethane 15-SP [39]	94.5 ± 12.7	2	6178 ± 510	2	1.5 ± 0.00	2
Urethane 15-55 [39]	95.1 ± 20.7	6	4613 ± 841	6	2.5 ± 0.53	6

N = number of samples tested.

Table A.4: Resin properties at LH_2 temperature

Resin ID	UTS (MPa)	N	E (MPa)	N	$\varepsilon_{failure}$ (%)	N
HEI 535 [35]	103.4 ± 7.6	3	8260 ± 1207	3	1.3 ± 0.07	2
Urethane 15-55 [39]	137.9 ± 14.5	3	7081 ± 669	3	2.0 ± 0.27	2

N = number of samples tested.

Table A.5: Strength of 2.5 cm wide NOL Rings with various resins and IM7 fiber [43]

Resin	Apparent Hoop Tensile Strength (MPa)		
	298 K	77 K	20 K
HEI 535 [35]	2194 ± 106	3214 ± 104	2721 ± 503
EPON 862/W [36]	2698 ± 137	2536 ± 325	2437 ± 542
CTD 7.1 [38]	2104 ± 131	2349 ± 270	2331 ± 214
Urethane 15-SP [39]	2026 ± 81	2823 ± 287	2573 ± 312
Urethane 15-55 [39]	2006 ± 34	2912 ± 485	3014 ± 325

Table A.6: Strength of 2.5 cm wide NOL rings with various resins and IM7 fiber with various sizings tested at ambient conditions

Resin	Fiber	UTS (MPa)	N
HEI 535 [35]	IM7 w/ No Sizing	1697 ± 41	5
	IM7 w/ 755 Sizing	1696 ± 42	5
	IM7 w/ 828 Sizing	1519 ± 22	5
Urethane AK423 [39]	IM7 w/ No Sizing	1493 ± 74	5
	IM7 w/ 755 Sizing	1785 ± 31	5
	IM7 w/ 828 Sizing	1754 ± 184	5

N = number of samples tested.

Table A.7: Strength of 2.5 cm wide NOL rings with various resins and IM7 fiber with various sizings tested at LN_2 conditions

Resin	Fiber	UTS (MPa)	N
HEI 535 [35]	IM7 w/ No Sizing	2127 ± 558	5
	IM7 w/ 755 Sizing	2658 ± 153	5
	IM7 w/ 828 Sizing	2722 ± 79	5
Urethane AK423 [39]	IM7 w/ No Sizing	2643 ± 99	5
	IM7 w/ 755 Sizing	2678 ± 156	5
	IM7 w/ 828 Sizing	2988 ± 137	5

N = number of samples tested.

Table A.8: T-1000/HEI 535 composite strength comparison for 0.9 cm and 2.5 cm wide NOL rings

	Ambient UTS (MPa)	LN_2 UTS (MPa)	N
NOL Ring (0.9 cm)	2387 ± 104	3431 ± 185	5
NOL Ring (2.5 cm)	2575 ± 130	3304 ± 265	5

N = number of samples tested.

Table A.9: T-1000/Epon 828/W composite strength comparison for 0.9 cm wide NOL ring and straight-sided specimens at ambient conditions

	Predicted UTS (MPa)	Actual UTS (MPa)	DFS (MPa)	N
NOL Ring (0.9 cm)	4838	2987 ± 86	4007 ± 116	5
Straight-sided	4115	2351 ± 204	3731 ± 324	5

N = number of samples tested.

Table A.10: T-1000/Epon 828/W composite strength comparison for 0.9 cm wide NOL ring and straight-sided specimens at LN_2 conditions

	Predicted UTS (MPa)	Actual UTS (MPa)	DFS (MPa)	N
NOL Ring (0.9 cm)	5020	2912 ± 86	3909 ± 114	5
Straight-sided	4276	1936 ± 182	2904 ± 267	5

N = number of samples tested.